

## A Novel 4 DoFs (3T-1R) Parallel Manipulator with Actuation Redundancy - Workspace Analysis

Samah Shayya, Sébastien Krut, Olivier Company, Cédric Baradat, François Pierrot

### ► To cite this version:

Samah Shayya, Sébastien Krut, Olivier Company, Cédric Baradat, François Pierrot. A Novel 4 DoFs (3T-1R) Parallel Manipulator with Actuation Redundancy - Workspace Analysis. MeTrApp'2013: 2nd Conference on Mechanisms, Transmissions and Applications, Oct 2013, Bilbao, Spain. 17 (Mechanisms and Machine Science), pp.317-324, 2014, New Advances in Mechanisms, Transmissions and Applications. <<http://www.ehu.es/compmech/metrap-2013/>>. <10.1007/978-94-007-7485-8\_39>. <lirmm-00906202>

**HAL Id: lirmm-00906202**

**<https://hal-lirmm.ccsd.cnrs.fr/lirmm-00906202>**

Submitted on 19 Nov 2013

**HAL** is a multi-disciplinary open access archive for the deposit and dissemination of scientific research documents, whether they are published or not. The documents may come from teaching and research institutions in France or abroad, or from public or private research centers.

L'archive ouverte pluridisciplinaire **HAL**, est destinée au dépôt et à la diffusion de documents scientifiques de niveau recherche, publiés ou non, émanant des établissements d'enseignement et de recherche français ou étrangers, des laboratoires publics ou privés.

# A Novel 4 DoFs (3T-1R) Parallel Manipulator with Actuation Redundancy – Workspace Analysis

Samah SHAYYA <sup>(a)</sup>, Sébastien KRUT <sup>(b)</sup>, Olivier COMPANYY <sup>(b)</sup>, Cédric BARADAT <sup>(a)</sup>, and François PIERROT <sup>(b)</sup>

(a)- TECNALIA FRANCE– MIBI Building, 672 Rue du Mas de Verchant, 34000 Montpellier, France- [www.tecnalia.com](http://www.tecnalia.com)

(b)-LIRMM –Université Montpellier 2 - 161 rue Ada, 34095 Montpellier, France

E-mails: [samah.shayya/cedric.baradat@tecnalia.com](mailto:samah.shayya/cedric.baradat@tecnalia.com)

[krut/company/francois.pierrot@lirmm.fr](mailto:krut/company/francois.pierrot@lirmm.fr)

**Abstract.** This paper presents a novel 4 dofs (3T-1R<sup>1</sup>) parallel actuatedly redundant mechanism and its workspace analysis, based on a performance index involving velocity and force capabilities. The robot is capable of performing a half-turn<sup>2</sup> about the z axis. Moreover, having all of its prismatic actuators along one direction; the x motion is independent- only limited by the stroke of the prismatic actuators. The mechanism is characterized by elevated dynamical capabilities having its actuators at base.

**Key words:** Parallel mechanism, actuation redundancy, 4 dofs mechanism, large rotational capacity, velocity and force performance index.

## 1 Introduction

For most industrial applications (such as machining) 6 dofs are too much. Thus studies have been conducted regarding the synthesis of 3 dofs (3T), 4 dofs (3T-1R) and 5 dofs (3T-2R) parallel manipulators. In fact, regarding some tasks, 4 dofs (3T-1R) parallel manipulators are sufficient. In others, where another rotation is required it can be provided either by the table or by an additional actuator in series with the parallel mechanism. Many 3T-1R parallel manipulators exist in liter-

---

<sup>1</sup> 3T-1R: Three-translational degrees of freedom (dofs) and one rotational degree of freedom.

<sup>2</sup> Complete rotation is constrained by unavoidable collisions.

ature such as the famous Delta robot [2] (with the **R**-U-P-U<sup>3</sup> chain), the Kanuk [10], the SMG in [1], the H4 in [8], the I4 in [6], the Par4 in [7] with its industrialized version Adept Quattro [9] (fastest industrial pick-and-place robot). Also, an interesting family of fully-isotropic parallel 4 dofs (3T-1R) manipulators, in addition to decoupled manipulators, has been synthesized in [4]. In [4], there is an elaborated referencing to other 4 dofs manipulators.

However, these and other existing manipulators have some drawbacks. For example, in the case of Delta with a huge workspace (even much larger with linear Delta), the presence of the RUPU chain connecting the base to the platform to supply the rotational dof is a weak element reducing the workspace. Others present problems of singularities, limitation of workspace (and particularly) in rotational capability, complexity of obtaining analytical expressions for the direct geometric model, and /or the use of transmission systems with the articulated platform as in the case [6-9] which impacts the accuracy of the robot. The manipulators in [4], despite their interesting isotropic property, have a limited workspace, are complex from manufacturability point of view, and have poor rigidity.

In this paper we present, a 4 dofs (3T-1R) parallel mechanism with two degrees of actuation redundancy that responds to the major requirements: large operational workspace, high rotational capability, absence of singularities, design simplicity, high rigidity, and high dynamical capabilities with analytical expressions for the inverse and direct geometric models. The paper introduces the mechanism in section 2, its geometrical elements, its inverse geometric model and the inverse jacobian matrix. Then section 3 describes the new performance index and workspace analysis of this mechanism. The paper ends with section 4 giving the conclusions.

## 2 The New 4 DoFs (3T-1R) Manipulator (ARROW)

The graph diagram of the four dofs (3T-1R) parallel mechanism, called **ARROW** (**A**ccurate **R**apid **R**obot with Large **O**perational **W**orkspace), is shown with its CAD drawing in Fig. 1. In Fig.2 we show the frontal view of the robot and platform details.

The robot consists of six actuators along the same direction (x-axis) and can perform four motions x, y, z and  $\Theta$  (rotation about z-axis). The robot is redundant (having two extra actuators). It is quite clear that this robot can move along x independently of the other motions y, z and  $\Theta$ . This motion along x is only limited by the available stroke for the prismatic actuators. The role of parallelograms in

---

<sup>3</sup> R, U, and P: correspond to rotational, universal, and prismatic joints. Bold faced letter means actuated, and underlined letter means the joint position is measured.

chains (III) and (IV) (see Fig. 2) is to constraint the platform rotation about any axis that is perpendicular to the z axis of the base frame.

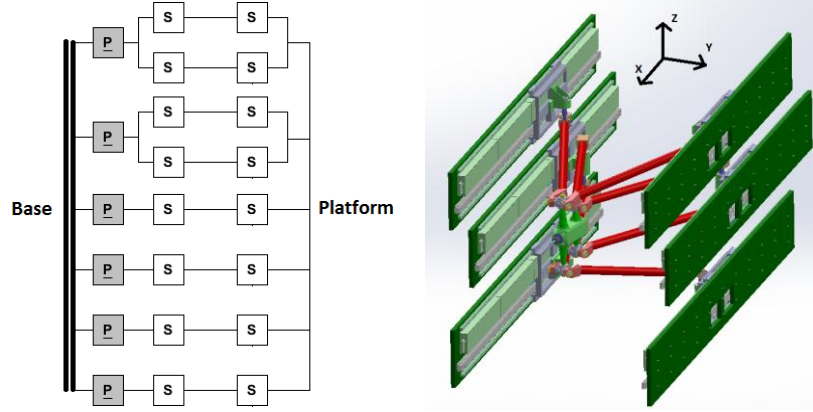


**Fig. 1** Graph diagram of the mechanism on the left and CAD drawing of the robot with its base frame on the right. P: prismatic joint, S: spherical joint<sup>4</sup>. Gray box means actuated, while white box means passive. The underlining signifies that the joint position is being measured.

These two parallelogram arms cooperate with the other four simple arms to position the TCP and control the platform orientation about the z axis.

Let  $L_i$  be the length of  $i^{\text{th}}$  arm  $A_i B_i$  (all simple arms are of equal length  $L_s$  and parallelogram arms of equal length  $L_p$ ) with  $A_i = (q_i \ y_i \ z_i)^T$  and  $B_i = (x_{b_i} \ y_{b_i} \ z_{b_i})^T$  in the base frame. Note that  $B_i^m = (x_{b_i}^m \ 0 \ z_{b_i}^m)^T$  in platform frame and the terms  $y_i$  and  $z_i$  can be determined from Fig. 2. Denote  $P = (x \ y \ z)^T$  (TCP coordinates) and the pose  $x = (x \ y \ z \ \theta)^T$  ( $\theta$  : rotation about z-axis). Then the inverse geometric model (IGM) is given by:

$$q_i = x_{b_i} - \sqrt{L_i^2 - (y_{b_i} - y_i)^2 - (z_{b_i} - z_i)^2}, \quad \forall i = 1 \dots 6 \quad (1)$$

$$B_i = P + R B_i^m, \quad \text{with } R = \begin{bmatrix} \cos(\theta) & -\sin(\theta) & 0 \\ \sin(\theta) & \cos(\theta) & 0 \\ 0 & 0 & 1 \end{bmatrix} \quad (2)$$

<sup>4</sup> Note that spherical joints practically can be replaced by three revolute joints as to overcome the problem of limited angular deviations in commercial spherical joints.

The inverse jacobian  $J_m$  is determined by equiprojectivity of velocities, giving

$$(\dot{q} = J_m v, v = (\dot{x} \quad \dot{y} \quad \dot{z} \quad \dot{\theta})^T, \dot{q} = (\dot{q}_1 \quad \dots \quad \dot{q}_6)^T)^5:$$

$$J_m = J_q^{-1} J_x; J_q = \text{diag}(A_1 B_1^T e_x, \dots, A_6 B_6^T e_x), J_x = \begin{bmatrix} A_1 B_1^T & -A_1 B_1^T (PB_1 \times e_z) \\ \vdots & \vdots \\ A_6 B_6^T & -A_6 B_6^T (PB_6 \times e_z) \end{bmatrix} \quad (3)$$

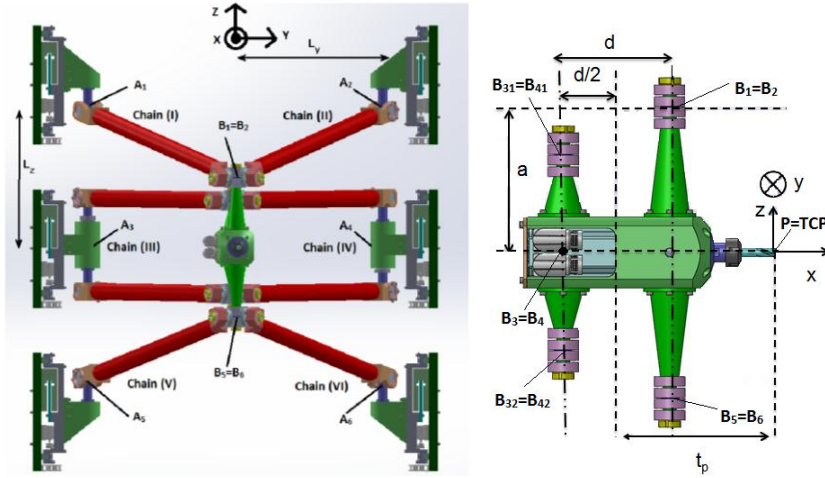


**Fig. 2** Frontal view of the robot on the left and platform details on the right (TCP at origin of base frame with zero rotation). The  $L_y$  and  $L_z$  are related to  $y_i$  and  $z_i$  coordinates of point  $A_i$ . Note that chains (III) and (IV) are parallelograms. The points  $A_3$  and  $B_3$  are along the virtual axis of parallelogram (III) (mid-line). The same applies for chain (IV). The TCP (tool center point) is shown also and is denoted by P and it is the origin of the platform moving frame.

The singularity analysis (although is not discussed here in details due to space limitation) shows that if the mechanism is to have parallel type singularities they are necessary coincident with serial type singularities which cannot take place except at the boundary of the geometrically accessible workspace (when one of the arms happens to be in the  $yz$  plane provided that the corresponding pose is geometrically accessible). Hence, we can assure that there are no singularities of any type (serial or parallel) within the geometrically accessible workspace excluding its boundary.

---

<sup>5</sup> Note that  $\dot{f} = \frac{df}{dt}$  is the time derivative of a function  $f(t)$ . Note also that  $e_x$ ,  $e_y$  and  $e_z$  are the unit vectors along x, y, and z axes of the base frame.

### 3 Workspace Analysis

The workspace analysis can be limited to investigating the yz region that allows a half-turn (or a certain range of rotation) and where the value of the chosen performance index is within the acceptable range. There are several indices in literature that might be used to evaluate the robot's performance [5, 11, 12] and each has its own limitations. However, in our case, we are interested in assuring a certain minimal kinetostatic performance in all directions; more precisely assuring a minimal speed capability while being capable at the same time of supporting a minimal external force, regardless of the velocity or force direction. The robot under study being redundant, the singular values of the jacobian matrix are no longer significant regarding this aspect and so is the condition number based on the ratio of largest singular value to the minimal one. So, in our study and evaluation of the workspace, we have defined the following index:

$$FVI = \min \left( \frac{v_w}{v_{wl}}, \frac{f_w}{f_{wl}} \right) \quad (4)$$

The terms  $v_w$  and  $f_w$  are the worst speed and the worst force respectively, whereas  $v_{wl}$  and  $f_{wl}$  are the desired lower bounds for the worst speed and worst force (not inducing internal stresses), respectively. Actually,  $v_w$  is nothing except the largest isotropic speed (radius of the largest sphere included in the zonotope of the operational velocities), and  $f_w$  is similarly the largest isotropic force (radius of largest sphere included in the operational force zonotope not inducing internal stresses). In our case, we have chosen  $v_{wl} = 0.25 \dot{q}_{\max}$  and  $f_{wl} = 0.25 \tau_{\max}$ . The terms  $\dot{q}_{\max}$  and  $\tau_{\max}$  are respectively the maximum speed and maximum force of the linear actuator (all actuators are considered identical).

Since we have mixed dofs (translation and rotation), it is mandatory to homogenize  $\mathbf{J}_m$  before evaluating the index at each pose if we are interested in all dofs (as to detect singularity while evaluating kinetostatic analysis)<sup>6</sup>. For this purpose, we may use a suitable characteristic length... However, in our case, we are only interested in the translational dofs (x, y and z motions), so we will consider only the translational part of  $\mathbf{J}_m$ , call it  $\mathbf{J}_{mp}$  composed of the first three columns of  $\mathbf{J}_m$ . Note that this would not be sufficient unless a separate singularity analysis prior to this has been made and it is our case here (the study is not included here due to space limitation, but it is done). The terms  $v_w$  and  $f_w$  are given by:

---

<sup>6</sup> Note that we can show that when  $v_w = 0$ , we have serial-type singularity and when  $f_w = 0$  we have parallel-type singularity. So the closeness of  $FVI$  to zero can serve as a singularity measure as well.

$$v_w = \min_{i=1\dots 6} \left( \frac{1}{\|\mathbf{j}_{mpr_i}\|} \right) \dot{q}_{\max}, f_w = \min_{i=1\dots 6} \left( \frac{1}{\|\mathbf{j}_{pc_i}\|} \right) \tau_{\max} \quad (5)$$

The terms  $\mathbf{j}_{mpr_i}$  and  $\mathbf{j}_{pc_i}$  mean the  $i^{\text{th}}$  row vector of matrix  $\mathbf{J}_{mp}$  and  $i^{\text{th}}$  column vector of the matrix  $\mathbf{J}_p$ , the pseudo-inverse of  $\mathbf{J}_{mp}$ . The proof of Eq. (5) is similar to the proof of the dynamic index introduced in [3].

In what follows we have established the yz region with zero orientation ( $\theta = 0^\circ$ ) and the yz region with rotation  $\theta \in [-45^\circ \ 45^\circ]$  despite the fact that the robot can produce half-turn ( $\pm 45^\circ$  being sufficient for our application) (see Fig. 3). Regarding the case of yz region with rotation, we have evaluated *FVI* for a set of different rotational angles particularly  $\pm 45^\circ, \pm 30^\circ$  and  $0^\circ$  for the purpose of reducing computation time and we assumed the worst value of this index for the corresponding  $(y, z)$  position (in this case the minimal value of *FVI*). For this study, we used the following optimized parameters:  $L_s = 0.72m$ ,  $L_p = 0.86m$ ,  $L_y = 0.35m$ ,  $L_z = 0.314m$ ,  $d = 0.12m$ ,  $a = 0.164m$ , and  $t_p = 0.18m$ .

Notice that the robot has its workspace symmetric with respect to xz and yz planes, and convex. The latter property, namely convexity, is very advantageous regarding trajectory planning; any two points in the workspace can be connected by a straight line trajectory.

To avoid collision with slider guides, the TCP should be at least at a distance  $t_l = 0.2m$  in case of rotation  $\pm 45^\circ$  and at a distance  $t_w = 0.073m$  in case of zero rotation. Note that  $t_w$  and  $t_l$  are generally imposed by the platform dimensions, spindle motor and tool size. These plots show that the yz region with and without orientation is large, especially when we consider the available space between its slider guides and collision limits with the sliders, which is quite interesting.

For better insight on the results regarding the workspace areas and variations of the index, we have tabulated them (see Table 1).

## 4 Conclusions and Future Work

In this paper, we have presented a new 4 dofs (3T-1R) parallel redundant mechanism (**ARROW**). It has 6 actuators for 4 dofs; the interest in this actuation redundancy is eliminating singularities and improving performance. The geometric models and inverse jacobian were derived. Singularity analysis results were briefed due to space limitation. We have then calculated the different workspaces and presented a new kinetostatic performance index “*FVI*” which is suitable for redundant and non-redundant robots equally well.

The workspace of this mechanism along x direction is independent of the other motions and only limited by the available stroke of the linear actuators, which is

one of its major advantages. The yz accessible regions are large in both cases with and without orientation, especially when compared to the space between its slider guides. The mechanism is particularly interesting having the capability to perform a half-turn (complete rotation is not possible due to unavoidable collisions).

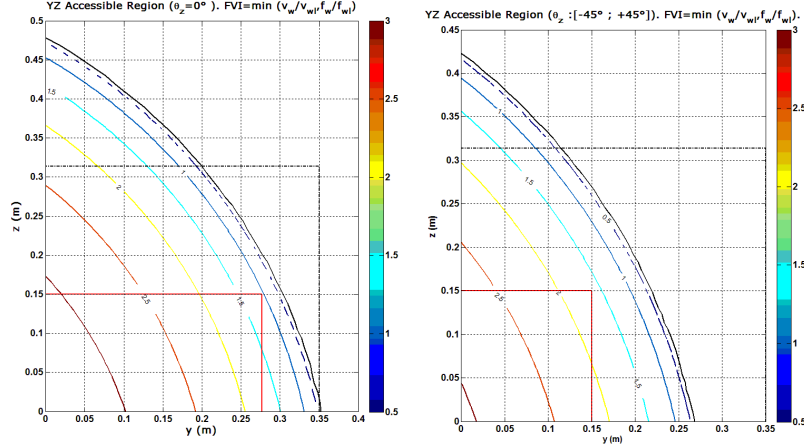


**Fig. 3** Accessible yz regions for  $\Theta=0^\circ$  (left) and for  $\Theta$  between  $-45^\circ$  and  $+45^\circ$  (right): quarter of the region is shown since it is symmetric with respect to y-axis and z-axis. The red solid lines show the boundaries that should not be exceeded by the TCP to avoid collisions with the sliders (vertical red line) and inter-arm collisions (horizontal red lines). Dotted black line shows the available space within the linear sliders.

**Table 1:** Workspace analysis and FVI index variations over the workspace.

		Area (m <sup>2</sup> )	Area/(4*L <sub>y</sub> *L <sub>z</sub> )	Mean Value	Standard Deviation
Collisions not considered	Workspace $\Theta=0^\circ$ (no limits)	0.441	1.00	2.01	0.76
	Workspace $\Theta=0^\circ$ (FVI $\geq$ 1)	0.387	0.88	2.19	0.62
	Workspace $\Theta:\pm 45^\circ$ (no limits)	0.288	0.65	1.79	0.70
	Workspace $\Theta:\pm 45^\circ$ (FVI $\geq$ 1)	0.243	0.55	2.00	0.53
Collisions considered	Workspace $\Theta=0^\circ$ (no limits)	0.165	0.38	2.55	0.52
	Workspace $\Theta=0^\circ$ (FVI $\geq$ 1)	0.165	0.38	2.55	0.52
	Workspace $\Theta:\pm 45^\circ$ (no limits)	0.089	0.20	2.48	0.31
	Workspace $\Theta:\pm 45^\circ$ (FVI $\geq$ 1)	0.089	0.20	2.48	0.31

Besides, having the arms connected to the platform and actuators via spherical joints, puts these arms under tension/compression forces making it easier to model deformation and compensate for it. In brief the simplicity of the design, the actuation redundancy, the actuation at base, and the high stiffness of the mechanism



contribute to the high dynamical capabilities (regarding pay-load, acceleration and velocity) as well as to its enhanced performance regarding accuracy. Regarding the future work, the introduced robot is currently being under further study (regarding dynamics) and under optimization in the sense of implementing it and producing a prototype on which real performance can be evaluated.

## Acknowledgement

This work has been supported partially by the French National Research Agency within the ARROW project (ANR 2011 BS3 006 01) and by Tecnalía France.

## References

1. Angeles J., Caro S., Khan W., Morozov A., « The kinetostatic design of an innovative Schonflies-motion generator », Proceedings of the Institution of Mechanical Engineers, Part C: Journal of Mechanical Engineering Science 220 (7) (2006) 935–943.
2. Clavel R., “Une nouvelle structure de manipulateur parallèle pour la robotique légère », *APII*, 23(6), 1985, pp. 371-386.
3. Corbel D., Gouttefarde M., Company O., and Pierrot F., “Towards 100G with PKM. Is actuation redundancy a good solution for pick-and-place?” 2010 IEEE International Conference on Robotics and Automation, Anchorage, Alaska, USA, May 3-8, 2010.
4. Gogu G., “Structural synthesis of fully-isotropic parallel robots with Schonflies motions via theory of linear transformations and evolutionary morphology”, *European Journal of Mechanics A/Solids* 26 (2007) 242-269.
5. Gosselin C. and Angeles J., “Global performance index for the kinematic optimization of robotic manipulators”, *Transaction of the ASME, Journal of Mechanical Design*, Vol. 113, no. 3, pp. 220-226, 1991.
6. Krut S., Company O., Benoit M., Ota H., and Pierrot F., “I4: A new parallel mechanism for Scara motions,” in Proc. of the 2003 Int. Conf. on Robotics and Automation, Taipei, Taiwan, September 2003, pp. 1875–1880.
7. Nabat V., Company O., Krut S., Rodriguez M., and Pierrot F., “Par4: very high speed parallel robot for pick-and-place”, in Proc. IEEE International Conference on Intelligent Robots and Systems (IROS’05), Edmonton, Alberta, Canada, August 2005.
8. Pierrot F., Company O., H4: a new family of 4-dof parallel robots, In: Proc. of the IEEE/ASME Int. Conf. on Advanced Intelligent Mechatronics, Atlanta, USA, 1999, pp. 508–513.
9. Pierrot F., Nabat V., Company O., Krut S., “From Par4 to Adept Quattro”, in Proc. Robotic Systems for Handling and Assembly - 3rd International Colloquium of the Collaborative Research Center SFB 562, Braunschweig, Germany, (2008).
10. Rolland L., “The Manta and the Kanuk: Novel 4 dof parallel mechanism for industrial handling”, in Proc. of ASME Dynamic Systems and Control Division IMECE’99 Conference, Nashville, USA, November 14-19, 1999, vol. 67, pp. 831-844.
11. Salisbury J. K. and Craig J. J., “Articulated hands: force control and kinematic issues”, *International Journal of Robotics Research*, Vol. 1, no. 1, pp. 4-17, 1982.
12. Yoshikawa T., “Manipulability of robotic manipulators”, *International Journal of Robotics Research*, Vol. 4, no. 2, pp. 3-9, 1985.